

1 **Rubber plant root properties induce contrasting soil aggregate stability**
2 **through cohesive force and reduced land degradation risk in southern China**

3 Waqar Ali¹, Amani Milinga ¹, Tao Luo², Mohammad Nauman Khan³, Asad Shah³, Khurram
4 Shehzad⁵, Qiu Yang¹, Huai Yang⁴, Wenxing Long¹, Wenjie Liu^{1*}

5 ¹*Center for Eco-Environment Restoration Engineering of Hainan Province, School of Ecology,*
6 *Hainan University, Haikou, 570228, China.*

7 ²*CSIRO Agriculture and Food, Private Bag 5, Wembley, WA 6913, Australia.*

8 ³*School of Breeding and Multiplication (Sanya Institute of Breeding and Multiplication), Hainan*
9 *University, Haikou, 570228, China*

10 ⁴*Institute of Tropical Bamboo, Rattan & Flower, Sanya Research Base, International Center for*
11 *Bamboo and Rattan, Sanya 572000, China*

12 ⁵*Hubei Key Laboratory of Soil Environment and Pollution Remediation, College of Resources and*
13 *Environment, Huazhong Agricultural University, Wuhan, 430070, China*

14

15

16 * **Corresponding authors:** Wenjie Liu

17 E-mail: liuwj@hainanu.edu.cn

18 Tel: 86-17733181789

19

20 **Abstract**

21 In southern China, Hainan Island faces land degradation risks due to a combination of soil
22 physical, chemical, and climatic factors. Specifically, soil physical properties like a high
23 proportion of microaggregates (<0.25 mm), chemical properties such as low soil organic matter
24 (SOM) content, and a climatic factor of frequent uneven rainfall. The cohesive force between soil
25 particles, which is influenced by plant root properties and root-derived SOM, is essential for
26 improving soil aggregate stability and mitigating land degradation. However, the mechanisms by
27 which rubber plant root properties and root-derived SOM affect soil aggregate stability through
28 cohesive forces in tropical regions remain unclear. This study evaluated rubber plants of different
29 ages to assess the effects of root properties and root-derived SOM on soil aggregate stability and
30 cohesive forces. Older rubber plants (> 11 -years-old) showed greater root diameters (RD) (0.81–
31 0.91 mm), higher root length (RL) densities (1.83–2.70 cm cm⁻³), and increased proportions of fine
32 (0.2–0.5 mm) and medium (0.5–1 mm) roots, leading to higher SOM due to lower lignin and higher
33 cellulose contents. Older plants exhibited higher soil cohesion, with significant correlations among
34 root characteristics, SOM, and cohesive force, whereas the random forest (RF) model identified
35 aggregates (> 0.25 mm), root properties, SOM, and cohesive force as the key factors influencing
36 mean weight diameter (MWD) and geometric mean diameter (GMD). Furthermore, partial least
37 squares-path models (PLS-PM) showed that the RL density (RLD) directly influenced SOM (path
38 coefficient 0.70) and root-free cohesive force (RFCF) (path coefficient 0.30), which subsequently
39 affected the MWD, with additional direct RLD effects on the SOM (path coefficient 0.45) and
40 MWD (path coefficient 0.64) in the surface soil. Cohesive force in rubber plants of different ages
41 increased macroaggregates (> 0.25 mm) and decreased microaggregates (< 0.25 mm), with topsoil
42 average MWD following the order: Control (CK) (0.98 mm) $<$ 5Y_RF (1.26 mm) $<$ MF (1.31 mm)

43 < 11Y_RF (1.36 mm) < 27Y_RF (1.48 mm) < 20Y_RF (1.51 mm). Rubber plant root traits
44 enhance soil aggregate stability and mitigate land degradation risk in tropical regions, offering
45 practical soil restoration strategies through targeted root trait selection to strengthen soil cohesion,
46 ensure long-term agricultural productivity, and preserve environmental quality, highlighting the
47 need for further research across diverse ecological zones and forest types.

48 **Keywords:** Rubber plant root traits; soil organic matter; cohesive force; aggregate stability; land
49 degradation

50 **1. Introduction**

51 Land degradation is a serious global issue that increases as a consequence of growing
52 population and climate change, currently impacting > 75% of land and projected to affect > 90%
53 by 2050 (Perović et al., 2021; Prävālie et al., 2021; Thomas et al., 2023). Land degradation in
54 tropical regions, such as Hainan Island, southern China, is driven by unfavorable soil conditions,
55 including a high proportion of microaggregates (<0.25 mm) often observed in degraded soils due
56 to macroaggregate breakdown which reduces structural stability, water infiltration, and low soil
57 organic matter (SOM) content, which further weakens soil structure. Additionally, the uneven and
58 high frequency of rainfall events during the summer season (May–October), combined with global
59 climate change, further intensifies water erosion and accelerates land degradation (Shao et al.,
60 2024; Zhu et al., 2022). In addition, zonal ferro-alumina lateritic soils (ferralsols) on Hainan Island,
61 classified as having low resilience and sensitivity according to the tropical soil resilience-
62 sensitivity matrix, are particularly prone to soil erosion (Li et al., 2022). Consequently, the current
63 soil erosion area on Hainan Island has increased 4.8-fold compared to that in 2000, according to a
64 third national soil erosion remote-sensing survey (Yu et al., 2016). Soil aggregates are fundamental
65 to soil function, and their stability regulates carbon cycling, nutrient storage, soil fertility,

66 infiltration rate, and resistance to soil degradation (Hok et al., 2021; Rabot et al., 2018; Yudina and
67 Kuzyakov, 2023). Therefore, it is imperative to enhance soil aggregate stability by implementing
68 suitable management practices that protect the integrity of the environment and ensure sustainable
69 agricultural productivity.

70 Natural rubber (*Hevea brasiliensis*) plantations have recently expanded rapidly across
71 mainland Southeast Asia (Xu et al., 2023; Yang et al., 2024). Rubber plants are recognized for their
72 effectiveness in improving soil aggregate stability through their root properties and in mitigating
73 soil erosion (Kurmi et al., 2020; Sun et al., 2021). Root morphology, particularly traits like fine
74 roots length (FRL), coarse roots length (CRL), root diameter (RD), and root length density (RLD),
75 influences soil structure by enhancing particle binding. Fine roots, with their higher surface area,
76 increase root-soil contact, promoting stronger aggregate formation through entanglement and
77 cohesive force. Plant roots influence soil aggregate size distribution by promoting FRL, which
78 closely interacts with soil particles, and negatively affecting CRL, which disintegrates into larger
79 particles (Ali et al., 2022; Chen et al., 2021; Kumar et al., 2017). Plant morphological root traits,
80 such as RD and RLD, and their chemical composition, including lignin and cellulose content,
81 have been shown to alter carbon deposits in soil pools and their sequestration (Poirier et al., 2018b;
82 Rossi et al., 2020). Nevertheless, several studies have suggested that the interaction between soil
83 particles and plant root-derived SOM is limited, which significantly affects soil particle stability
84 through cohesive forces, particularly after root decomposition (Ali et al., 2022; Chen et al., 2017).
85 Variations in soil particles and root-derived SOM further adjust soil cohesion.

86 Soil cohesive forces, derived from SOM and the morphological and chemical properties of
87 plant roots (Wang et al., 2018a; Wang et al., 2020), effectively stabilize sloped soils by enhancing
88 soil-particle interactions, promoting flocculation, and minimizing soil erosion, thereby controlling

89 soil and water runoff (Smith et al., 2021; Wang et al., 2018a). Among these factors, SOM plays a
90 complex role and is generally beneficial for promoting particle flocculation. However, an excess
91 charge on SOM, combined with the negative charges of soil particles, can also lead to the
92 dispersion of aggregates (He et al., 2021; Melo et al., 2021). The addition of plants and their roots
93 allows for additional soil organic carbon (SOC) accumulation in the soil (Rossi et al., 2020). Roots
94 can also bind soil particles via cohesive forces, thus increasing aggregate stability (Forster et al.,
95 2022; Poirier et al., 2018a; Wang et al., 2020). Dominant root traits influence soil particles through
96 cohesive forces, and their subsequent effects on soil aggregate stability remain unknown.

97 So far, few studies have investigated the impact of rubber plant roots on soil aggregation
98 in the tropical region of Hainan Island (Sun et al., 2021; Zou et al., 2021), and there is a complete
99 lack of research regarding the mechanisms related to rubber plant root morphological and chemical
100 properties, root-derived SOM, and cohesive forces in aggregate formation. We hypothesized that
101 rubber plantations of different stand ages would promote soil cohesive forces through root
102 properties and SOM among soil particles, ultimately improving aggregate stability. This study
103 aimed to: 1) investigate the impact of stand-age rubber plant root traits and root-derived SOM on
104 aggregate properties, and 2) explore the interconnections between root morphological and
105 chemical characteristics, SOM, cohesive forces, and soil aggregate stability. The findings of this
106 research will contribute to better management practices in the tropical regions of Hainan Island,
107 helping to mitigate land degradation issues by enhancing aggregate stability and overall
108 environmental quality.

109 **2. Materials and methods**

110 *2.1. Experimental site overview*

111 The study was conducted on Hainan Island in Danzhou (19°4'3''–19°12'42''N, and 109°47'
112 6''–110°1'2''E, 182–255 m above sea level). In the study area, the annual averages for temperature,
113 precipitation, and solar radiation are 23.5°C, 1831 mm, and 4579 MJ·m⁻²·yr⁻¹, respectively.
114 November–April of the following year is the dry season, whereas May–October is the rainy season.
115 Rubber (*Hevea brasiliensis*) and areca (*Areca catechu* L.) are the two primary commercial crops
116 in the experimental region. Prior to rubber plantation, the land was covered by tropical rainforest.
117 According to the USA Soil Taxonomy System, the soil is classified as a laterite ferralsol (Schad,
118 2023). The soil in the rubber plantation was composed of 43.71% sand, 8.28% silt, and 48.01%
119 clay. The basic physical and chemical characteristics of the samples are listed in Table. 1.

120 2.2. Experimental design

121 Rubber plantations with four different stand ages were selected from the field. The
122 treatments included five-year-old rubber forests (5Y_RF), with 2018 rubber trees (clone PR-107)
123 planted at the recommended density (3 × 7 m, 480 plants·ha⁻¹) and crown density 30 %; 11-year-
124 old rubber forests (11Y_RF), with 2012 rubber trees (clone PR-107) planted at the recommended
125 density (3 × 7 m, 431 plants·ha⁻¹) and crown density 90 %; 20-year-old rubber forests (20Y_RF),
126 with 2003 rubber trees (clone PR-107) planted at the recommended density (3 × 7 m, 346
127 plants·ha⁻¹) and crown density 90 %; 27-year-old rubber forests (27Y_RF), with 1996 rubber trees
128 (clone PR-107) planted at the recommended density (3 × 7 m, 300 plants·ha⁻¹) and crown density
129 90 %; and mixed forest (MF) and control (no forest plants) (CK). The MF treatment represents a
130 mixed forest system consisting of cinnamon (*Cinnamomum verum*) trees (planted in 2014)
131 intercropped with 20-year-old rubber (*Hevea brasiliensis*) trees. This treatment was included to
132 assess the potential benefits of mixed-species plantations on soil aggregation and stability
133 compared to monoculture rubber plantations. We established a randomized complete block design

134 with three replicates. We selected 18 plots (30×30 m) separated by a transitional zone. Rubber
135 plants with different stand ages were selected based on similar topographies (slope and gradient)
136 and management practices. Rubber plantation canopy heights were approximately 20 m. The
137 rubber plant rotation duration was approximately 40 yr, and the first latex tappings in this region
138 occurred when the trees were five- or six-years-old. Chemical fertilizers were applied at the initial
139 rubber plantation development stage according to local conventional farming practices. Additional
140 details regarding the rubber plantations at the experimental site can be found in the study by Sun
141 et al. (2021).

142 *2.3. Root morphological and chemical composition analysis*

143 In January 2024, three replications per depth per forest plot of soil samples with roots were
144 taken at soil depths of 0–20 and 20–40 cm, using cutting rings (200 cm^3). Using the methodology
145 outlined by Chen et al. (2021), the following root features were measured: RD, root mass density
146 (RMD), RLD, and root surface area density (RSD). The cutting ring cores were placed in nylon
147 bags and taken to the laboratory, where they were submerged in water for an hour before being
148 manually washed using 0.55-mm sieves to collect the roots. The roots were scanned using an
149 Epson Perfection V800 photo scanner (© 2024 Epson America, Inc), and WinRHIZO Pro Version
150 2009c software was used to assess the RD and RL. By dividing the entire RL and root surface area
151 by the cutting-ring volume (cm^3), respectively, the RLD and RSD were calculated. The roots were
152 oven-dried at 50°C , and the RMD was calculated by dividing the dry root mass by the cutting-ring
153 volume. Furthermore, using data from the WinRHIZO analyzer, the root system was classified into
154 four types based on RD: $\text{RD} < 0.2$ mm (very fine roots (VFRL)), $\text{RD} 0.2\text{--}0.5$ mm (fine roots
155 (FRL)), $\text{RD} 0.5\text{--}1$ mm (medium roots (MRL)), and $\text{RD} > 1$ mm (CRL).

156 Chemical composition (cellulose and lignin) analysis of the roots was performed on three
157 subsamples of the root classes (RD < 0.5, 0.5–1, and > 1 mm). Briefly, 1 mg of 65 °C oven-dried
158 root powder (< 0.5 mm) was mixed with 5 ml acetic acid and heated for 25 min, followed by three
159 deionized water washings and supernatant discarding. Subsequently, 10 ml of sulfuric acid (10%)
160 and 10 ml of potassium dichromic (0.1 mol L⁻¹) solutions were added, vortexed, and heated in a
161 100 °C water bath for 10 min. After cooling, 5 ml KI solution (20%) and 1 ml starch (0.5%) were
162 added, shaken for 10 min, and then titrated with 0.2 mol L⁻¹ sodium thiosulfate to determine
163 cellulose and lignin contents (Zhang et al., 2014).

164 2.4. Soil cohesive force determination

165 Soil samples of approximately 2000 g were collected from depths of 0–20 cm and 20–40
166 cm using a soil auger during the root collection process. The samples were carefully extracted,
167 combined, and sealed in plastic bags for transportation to the laboratory for further analysis. Soil
168 samples were air-dried and divided into two parts. One part was ground to 100 µm for SOM
169 determination using the oxidation method described by Walkley and Black (1934). The second
170 part was dry-sieved to retain aggregates < 5 mm, and visible roots were removed. These soil
171 samples were stored for subsequent analysis of the remolded soil root-free cohesion force (RFCF),
172 which was determined according to the method described by Huang et al. (2022). Briefly, four
173 subsamples for root soil composite cohesive force (RSCCF) were collected from each depth in
174 three replicated plots using cutting rings (diameter = 10 cm, height = 6.37 cm) simultaneously
175 during the root collection described in Section 2.3. These intact cores were used to determine soil
176 cohesive forces. Soil cohesive force (c) was measured by assessing soil shear strength (τ) and
177 vertical load (σ) applied to the shear surface, and c was calculated using the relationship between
178 τ , σ , and c as described in Equation 1. In addition, soil (< 5 mm) without visible roots was remolded

179 into cutting rings (diameter = 10 cm, height = 6.37 cm) according to the soil bulk density (Table
180 1) at each soil depth in the rubber plots to measure the soil RFCF. In total, 48 core soil samples
181 per treatment were used for soil cohesive force analysis. Both the RFCF and RSCCF samples were
182 saturated with deionized water. After saturation, four subsamples from each depth and treatment
183 were tested using an LH-DS-4 direct shear tester (Nanjing Technology Co., Ltd.), which has a
184 shear strain accuracy of 0.01 mm and a shear stress accuracy of 0.01 N. The shear tester comprised
185 a shear box, a sensor, a vertical compression device, and a displacement measurement system with
186 specifications of 61.8 mm in diameter and a height of 20 mm. For the direct shear tests, four
187 predetermined vertical loads (25, 50, 75, and 100 kPa) were applied. The shear rate of displacement
188 was set at 0.8 mm min⁻¹, and the soils were sheared until failure, indicated by reaching the peak τ
189 value on the computer. The relationship between the peak τ values and vertical loads (σ) was
190 established according to Mohr–Coulomb’s law, and soil cohesion (c) was calculated as described
191 in Equation 1.

$$\tau = c + \sigma \tan\phi \quad (1)$$

192 where τ is the soil shear strength (kPa), σ is the vertical load applied to the shear surface (kPa), c
193 is the soil cohesive force (kPa), and ϕ is the soil internal friction angle (°).

195 2.5. Soil aggregate analysis

196 Soil samples from depths of 0–20 and 20–40 cm were collected in each treatment
197 simultaneously with the root sample collection. The soil was allowed to air dry and then gently
198 ruptured along its natural cracks before it was passed through an 8 mm mesh sieve to determine
199 the soil aggregate size distribution and stability. We used a wet sieving method to separate
200 aggregates < 8 mm into four size groups: large macroaggregates (LMA) (> 2 mm);
201 macroaggregates (MA) (2–0.25 mm); microaggregates (MIA) (0.25–0.053 mm); and small

202 microaggregates (SMA) (< 0.053 mm). Briefly, three replicates of 100 g of soil were immersed in
203 deionized water for 10 min in a beaker before being transferred to a series of sieves with decreasing
204 mesh sizes (2, 0.25, and 0.053 mm) and gently shaken in water with a 4-cm vertical vibration
205 amplitude for 10 min. Subsequently, the soil that remained after each sieve was washed
206 and transferred to a beaker, and all aggregate sizes (> 2, 2–0.25, and 0.25–0.053 mm) were oven-
207 dried for 48 hours at 60 °C before being weighed. The mass of aggregates < 0.053 mm was
208 determined by subtracting the total soil mass from the total mass of other aggregate sizes (Elliott,
209 1986). Equations 2 and 3 were used to compute the mean weight diameter (MWD, mm and
210 geometric mean diameter (GMD), respectively (Kemper and Rosenau, 2018).

211
$$MWD = \sum_{i=1}^n W_i * X_i \quad (2)$$

212 where X_i denotes the mean diameter of aggregate fraction i , and W_i denotes the mass proportion of
213 aggregate fraction i .

214
$$GMD = \exp [\sum_{i=1}^n W_i * \ln (X_i)] \quad (3)$$

215 where W_i represents the aggregate fraction mass proportion i , and X_i represents the mean diameter
216 of aggregate fraction i .

217 2.6. Statistical analysis

218 Shapiro–Wilk ($p > 0.05$) and Levene's tests ($p > 0.05$) (Razali and Wah, 2011) were used
219 to evaluate the normality and homogeneity of variances using SPSS 25 (IBM Corp., Chicago,
220 USA). Origin 2021 software was used to evaluate each index. One-way analysis of variance
221 (ANOVA) was conducted to determine statistical significance at $p < 0.05$, followed by Tukey's

222 test to assess treatment significance. Pearson's correlations among root characteristics, SOM, soil
223 aggregate parameters, and soil cohesive force were assessed using Origin software (OriginLab
224 Corp.). The random forest (RF) model was constructed using the R software Random Forest
225 package (v4.3.1) (Team, 2017), with hyperparameters, including ntree, mtry, importance,
226 proximity, etc., to optimize through grid search and 5-fold cross-validation. The Gini index
227 assessed variable importance, and model performance was evaluated using MSE and R^2 on a 30%
228 validation dataset. The partial least squares-path models (PLS-PM) were performed in R software
229 (v4.3.1) using the "plspm" package to elucidate the bootstrapping (5,000 iterations) determined
230 significance of path coefficients ($*p* < 0.05$, 95% CIs). The R^2 and bootstrapped p-values
231 validated model adequacy through which plant root characteristics, SOM, and soil cohesive forces
232 influence soil aggregate stability. Figures were created using Origin 2021 (OriginLab Corp.).

233 **3. Results**

234 *3.1. Root distribution and chemical composition*

235 Significant differences in root morphological traits were observed among rubber
236 plantations of different stand ages (Fig. 1). The RD varied notably with the age of the rubber plant
237 (Fig. 1a). The largest RD was found in 27Y_RF, followed by the MF at depths of 0–20 cm and
238 20–40 cm, respectively. Specifically, the largest RD for 27Y_RF was 0.84 mm and 0.91 mm at
239 depths of 0–20 cm and 20–40 cm, respectively. By contrast, the smallest RD, found in five-year-
240 old rubber plantations (5Y_RF), ranged from 0.42 to 0.45 mm across both depths, respectively.
241 The differences in RD among rubber plants of varying stand ages depended on soil depth, with the
242 most significant differences found at the 0–20 cm depth. Furthermore, there were notable
243 variations in RLD between rubber plantations of different stand ages, as shown in Fig. 1b. The
244 27Y_RF exhibited the highest RLD, ranging from 1.83 to 2.81 cm cm^{-3} , followed by MF (2.01–

245 2.06 cm cm⁻³) and 20Y_RF (1.93–2.70 cm cm⁻³) at both depths. The RLD differences among
246 rubber plants of various stand ages were influenced by soil depth, with the most noticeable
247 differences occurring at a depth of 0–20 cm. In addition, the RSD and RMD were significantly
248 different among rubber plantations of different stand ages (Fig. 1c, and d). Furthermore, RD
249 distribution, represented as a percentage of RL within each RD class, also differed among rubber
250 plantations of various stand ages (Fig. 2). In the 5Y_RF, 11Y_RF, and MF plantations, VFRL (<
251 0.2 mm) predominated at both soil depths. Conversely, in the 20Y_RF and 27Y_RF plantations,
252 the roots were uniformly distributed across the soil depths, with a relatively high percentage of
253 MRL (0.5–1 mm).

254 The root chemical composition varied among rubber plantations of different stand ages and
255 RD classes (Fig. 3). The cellulose contents in stand-age rubber plants were significantly different
256 (Fig. 3a). The 20Y_RF roots had higher cellulose content than those of the 27Y_RF, followed by
257 the 11Y_RF. Similarly, cellulose content varied across the RD classes, with the 5Y_RF having
258 lower cellulose levels than other stand-age rubber plants for FRL (< 0.5 mm). Moreover, there
259 were significant differences in lignin content among the stand-age rubber plants and between the
260 RD classes (Fig. 3b). For example, the lignin contents in the 20Y_RF were less than that in the
261 5Y_RF for RL < 0.5 mm. Cellulose and lignin contents are indicators of root contribution to SOM.
262 Thus, the lower lignin and higher cellulose content in the 20Y_RF resulted in the highest SOM
263 content ranging from 21.16 to 23.37 g kg⁻¹, followed by that in the 11Y_RF, ranging from 20.56
264 to 22.68 g kg⁻¹, and the 27Y_RF ranging from 21.04 to 21.78 g/kg within soil depth (Fig. 3c).

265 3.2. Soil cohesive force under different stand-age rubber plantations

266 There was a significant difference in the RFCF among rubber plantations of different stand
267 ages (Fig. 4a). The CK (without plants) RFCF was 17.92 and 20.25 kPa at depths of 0–20 and 20–

268 40 cm, respectively, and the RFCF matrix significantly increased with the introduction of rubber
269 plantations of different stand ages. For example, at 0–10 cm soil depth, compared to the CK, the
270 ability of rubber plants to improve the soil cohesive force followed the order MF > 27Y_RF >
271 20Y_RF > 11Y_RF > 5Y_RF. For the 20Y_RF, the increases in RFCFs relative to the CK were
272 169.73 and 156 % at 0–20 and 20–40 cm, respectively. Generally, older rubber plants (> 11-years-
273 old) yielded a greater RFCF than younger rubber plants.

274 The root–soil composite cohesive force exhibited different patterns among rubber
275 plantations of different stand ages compared to that of the RFCF (Fig. 4b). The root–soil composite
276 cohesive force showed significant differences among rubber plantations of different stand ages and
277 with that in the CK at 0–20 cm depths, whereas the root–soil composite force was significantly
278 greater with plants than with that in the CK at 20–40 cm depth. However, there were no significant
279 differences in the root–soil composite cohesive forces among the different plantations within the
280 20–40 cm soil depth. This is likely because rubber plants of different stand ages (20Y_RF, 27Y_RF,
281 and MF) had greater root–soil interactions, likely due to thicker RD, higher RLD, higher
282 percentage of MRL, and higher SOM at a depth of 0–20 cm. Overall, both cohesive forces were
283 significantly correlated with RLD, VFRL, FRL, and SOM (Fig. 6). These results indicate that
284 rubber plantations of different stand ages have a greater ability to improve soil cohesive forces.

285 *3.3. Soil aggregate properties under different stand-age rubber plantations*

286 Soil aggregate properties exhibited different patterns among the various rubber plant
287 treatments (Fig. 5). Soil aggregates sizes were predominantly 2–0.25 mm, followed by > 2 mm,
288 and 0.25–0.053 mm, and aggregate sizes > 0.053 mm were less dominant in all rubber plantations
289 of different stand ages compared to that in the CK at the respective soil depths (Fig. 5a–f). In the
290 CK, the 2–0.025 mm aggregates accounted for 23.76% at a depth of 0–20 cm and 26.84% at 20–

291 40 cm. Compared to the CK, rubber plantations of different stand ages showed a significant
292 increase in 2–0.25 mm aggregates at both soil depths. However, the proportion of aggregates > 2
293 mm, significantly increased in rubber plantations of different stand ages compared to that in the
294 CK at respective soil depths, in the order 20Y_RF > 11Y_RF > 27Y_RF > MF > 5Y_RF.
295 Simultaneously, the proportion of aggregates < 0.053 mm was significantly reduced in rubber
296 plantations of different stand ages compared with the CK. The increase in macroaggregates (> 2
297 mm) and decrease in microaggregates (< 0.053 mm) following rubber plantation treatments of
298 varying stand ages led to improvements in aggregate stability (measured by MWD and GMD) in
299 the following order: 20Y_RF > 27Y_RF > 11Y_RF > MF > 5Y_RF > CK.

300 *3.4 Relationship among root traits, SOM, cohesive force, and soil aggregate stability*

301 The Pearson correlation analysis revealed a strong positive correlation between soil RFCF
302 and MWD as well as GMD, with correlation coefficients of 0.81 and 0.91 (0–20 cm) and 0.81 and
303 0.89 (20–40 cm). In contrast, soil RFCF showed a significant negative correlation with small
304 microaggregates (< 0.053 mm), with correlation values of –0.74 and –0.79 at both depths (Fig. 6).
305 A similar pattern was observed for the root–soil composite cohesive force. In general, a stronger
306 cohesive force was associated with higher RLD, greater proportions of FRL and MRL, and higher
307 SOM, especially in older rubber plants, which contributed to their ability to maintain greater
308 aggregate stability.

309 The Random Forest (RF) model highlighted the significance of various soil factors in
310 predicting soil aggregate stability (MWD and GMD) across both soil depths (Fig. 7), with LMA
311 (>2 mm) and MA (2–0.25 mm) emerging as the most influential contributors to stability, followed
312 by SOM and FRL (FRL_0.2–0.5 mm). Root properties and soil cohesive forces also play
313 substantial roles, particularly at deeper soil depths (20–40 cm), where cohesive forces become

314 more prominent. Furthermore, the PLS-PM clarified both the direct and indirect effects of root
315 properties, SOM, and cohesive forces on soil aggregate stability (Fig. 8). Among the factors
316 measured in the surface soil (0–20 cm), RLD (path coefficient 0.64, $P < 0.05$) directly influenced
317 SOM (path coefficient 0.45, $P < 0.05$) and the MWD. In addition, RLD had a strong direct effect
318 on SOM (path coefficient 0.70, $P < 0.05$). Furthermore, RLD directly altered RFCF (path
319 coefficient 0.30, $P < 0.05$), which further affected the MWD. In contrast, RLD directly influenced
320 the RSCCF, however, the RSCCF did not directly influence the MWD. A similar trend was
321 observed in the deep soil (20–40 cm).

322 **4. Discussion**

323 *4.1. Stand-age rubber plant roots influence on soil cohesive forces*

324 Rubber plantations of different stand ages exhibited different root morphological traits.
325 Our results demonstrated that the plant roots of rubber plantations aged < 11-years-old were
326 influenced by soil properties at 0–20 and 20–40 cm depths, as indicated by a sharp decline in RD
327 and RLD (Fig. 1), and restricted root growth due to an increase in soil bulk density and a decrease
328 in macropores. Similarly, Sun et al. (2021) observed that at the same research site, older rubber
329 plants (13-years-old) exhibited a preference for growing in macropores compared to younger
330 plants (four-years-old), which was attributed to their superior root properties and lower soil bulk
331 density. In contrast, the 27Y_RF and MF were minimally influenced by soil properties due to the
332 high percentage of FRL and MRL, which likely enlarged medium soil pores and facilitated
333 penetration through capillary soil pores ($< 30 \mu\text{m}$) (Ali et al., 2022; Chen et al., 2021; He et al.,
334 2022). Older rubber plants possess a higher proportion of FRL and MRL and produce a greater
335 amount of root exudates, which likely function as lubricants to facilitate root growth in compacted
336 soils with a higher bulk density (Chen et al., 2017; Sun et al., 2023). In our study, older rubber

337 plants demonstrated a higher root penetration ability than younger plants, which likely modified
338 the soil cohesive forces.

339 Our results indicate that rubber plant roots of different stand ages were more effective in
340 enhancing soil cohesive forces in tropical regions than in the CK (no rubber plants) (Fig. 4). Many
341 studies have highlighted that plant roots enhance soil detachment resistance during rainfall events,
342 primarily by increasing soil cohesive forces (Huang et al., 2022; Shen et al., 2021). Our findings
343 further confirm that rubber plantations of different stand ages generate varying soil cohesive forces,
344 which are influenced by their root properties and contributions to SOM. The differences in the
345 enhancement of root–soil composite cohesive forces among rubber plantations of varying stand
346 ages were attributed to their distinct root properties. Younger rubber plants (< 20Y_RF) were more
347 effective at increasing soil cohesion in the topsoil (0–20 cm), whereas older plants improved soil
348 cohesion in both the topsoil and deeper layers compared to that in the CK (Fig. 4) because of their
349 higher root tensile strength, soil shear strength, and greater RD and RLD. However, the RD and
350 RLD of younger plants were significantly reduced in the subsoil, thereby diminishing their impact
351 on soil cohesion. In contrast, older rubber plants enhance soil cohesive forces because of their
352 extensive root contact area with the soil and the high density of their crisscrossing FRL and MRL
353 networks, which effectively bind and wrap soil particles (Huang et al., 2022; Vannoppen et al.,
354 2015; 2017). In the current study, RLD and a substantial proportion of FRL and MRL in older
355 rubber plants enhanced root–soil contact and strengthened the soil at both depths (Figs. 1, and 2).

356 The impact of roots on the cohesive force of root-free soils can be attributed to their indirect
357 contribution to SOM. Soils from older rubber plantations, which exhibited higher SOM content
358 (Fig. 3c), enhanced clay particle cohesion by reducing the surface tension of water within the clay–
359 organic matter matrix (Wuddivira et al., 2009). RD and chemical composition (cellulose) altered

360 carbon sequestration in various soil pools, enhancing carbon accumulation in the coarse silt
361 fraction (20–50 μm), while decreasing carbon accumulation in particulate organic matter (Liao et
362 al., 2023; Zhang et al., 2014). Similarly, roots with higher cellulose-to-lignin ratios improve
363 substrate availability for polymer-hydrolyzing enzymes, thereby speeding up the degradation of
364 plant organic materials (Barto et al., 2010; Halder et al., 2021; Zhang et al., 2014). In addition,
365 root exudates facilitate root penetration into compacted soil layers and increase the distribution
366 frequency of SOM in deeper soil horizons (Oleghe et al., 2017). In general, older rubber plants
367 exhibited a greater RLD, higher percentage of FRL and MRL, and increased SOM than younger
368 rubber plants, which led to a higher RFCF.

369 *4.2. Aggregate stability responses to soil cohesive forces under different stand-age rubber* 370 *plantations*

371 Our study provides comprehensive insights into soil aggregate stability across rubber
372 plantations at different stages of stand maturity. Soil cohesive forces driven by plant root traits are
373 key factors in enhancing soil aggregate stability. The soil cohesive force increased aggregate
374 stability (MWD and GMD) at the same soil depth (Fig. 5). The root morphology traits like fine
375 FRL, CRL, RD, RLD, influence the soil cohesive force and binding of soil particles and then
376 indirectly increase aggregate stability (MWD and GMD). The results also indicated that cohesive
377 forces not only governed macroaggregate stability but also played a role in microaggregate
378 formation. Macroaggregates are primarily stabilized by cohesive forces derived from organic
379 matter, root exudates, and fungal hyphae. In our study, the significant increase in RFCF with the
380 introduction of rubber plantations (Fig. 4a) indicates that cohesive forces are enhanced by root
381 activity and organic matter inputs. Similarly, microaggregates are formed through the binding of
382 primary particles (clay, silt, and fine organic matter) by cohesive forces. In our study, the increased
383 RFCF in older plantations (Fig. 4a) suggests that cohesive forces are strong enough to facilitate

384 the formation of microaggregates, particularly in the topsoil (0–20 cm depth). The MWD increased
385 across rubber plantations of different stand ages because of the significant enhancement in soil
386 cohesive forces. Rubber plants older than 11 years exhibited the highest aggregate stability at the
387 same soil depth, which was consistent with the trend observed in their RFCF (Fig. 4). High soil
388 cohesion has also been documented to limit soil dispersion rates and mitigate gully erosion
389 (Wuddivira et al., 2013). Although the soil RFCCF was highest in older rubber plantations, the
390 highest SOM content likely played a positive role in stabilizing soil particles (Kamau et al., 2020).
391 SOM influences soil particles in several ways, primarily by enhancing soil aggregation and
392 improving soil structure. SOM contributes to the formation of aggregates by acting as a binding
393 agent between soil particles, especially through its interaction with clay minerals and other soil
394 constituents. The organic compounds in SOM help form cohesive forces that promote the
395 flocculation of fine soil particles, creating larger, more stable aggregates. SOM had a positive
396 effect on soil particles as its dispersive properties became evident only once the soil aggregates
397 were broken down. High SOM content also weakens the electrostatic repulsive forces by
398 influencing the overlap of oppositely charged electric double layers (Ali et al., 2023; Yu et al.,
399 2020). In addition, the higher MWD observed in rubber plantations older than 11 years, compared
400 to those in the 5Y_RF and CK, indicated that the MWD of older rubber plants was not adversely
401 affected by the excessive release of SOC from the mechanical breakdown of macroaggregates.
402 During this breakdown process, the enhanced root biomass and higher SOM content in older
403 rubber plantations help stabilize soil aggregates and mitigate the adverse effects of SOC loss.
404 Additionally, higher RLD and root-derived SOM in older plantations promote microaggregate
405 formation, further supporting aggregate stability and contributing to the observed increase in
406 MWD, despite the release of some SOC from macroaggregate breakdown.

407 These findings highlight the importance of understanding the specific mechanisms by
408 which soil cohesive forces contribute to aggregate stability. In this study, the soil aggregate portion
409 (< 0.25 mm) was comparatively higher in the rubber plantations than in the control in this study.
410 Rubber plant roots and SOM positively enhanced cohesion between soil particles (Fig. 5a–f). The
411 soil cohesive force regulates soil aggregate stability using the following approaches. First, smaller
412 aggregates, due to their higher surface area to volume ratio with water, can create surface tension
413 between particles, indirectly creating a cohesive force, helping to hold them together (Wang et al.,
414 2023). Second, soil particles, particularly clay and organic matter, often carry electrical charges
415 that can lead to electrostatic attraction, further stabilizing the soil particles (Kaiser and Asefaw,
416 2014; Wuddivira et al., 2009). SOM has a positive effect on clays because the dispersive effect of
417 SOM is not expressed until the aggregates are broken (Melo et al., 2021). High SOM also weakens
418 the electrostatic repulsive force in ultisols through its additional impact on the overlap of
419 oppositely charged electric double layers (Ali et al., 2023; He et al., 2021; Yu et al., 2020). Third,
420 the water in the small pores between the soil particles creates a capillary force that contributes to
421 the soil cohesive force, which agglomerates the small particles (Deviren Saygin et al., 2021). In
422 general, stand-age rubber plantations positively improved soil aggregate stability compared to the
423 control through soil cohesion. In young rubber plantations, legumes such as kudzu should be
424 planted. Furthermore, the development of a forest rubber understory economy can significantly
425 enhance soil health by increasing biodiversity, with diverse plant roots improving soil structure,
426 promoting microbial activity, preventing erosion, and contributing to organic matter through leaf
427 litter and root biomass, thereby improving soil fertility. Future research should focus on evaluating
428 the mechanisms by which various understory plants in rubber plantations reduce soil erosion.

429 **5. Conclusion**

430 In this study, we investigated how root morphological traits, root-derived SOM, and the
431 chemical composition of rubber plants at different stand ages influence soil aggregate stability
432 through soil cohesive forces. Our findings indicate that natural rubber plantations of different stand
433 ages exhibit distinct root distribution patterns, with older rubber plantations, particularly 27-year-
434 old rubber forests, and MF demonstrating a more developed root system characterized by greater
435 RLD and higher proportions of FRL and MRL diameter classes compared to younger plantations.
436 The higher percentages of FRL and MRL in older rubber plants (> 11 years old), along with their
437 high SOM content, contributed to a stronger soil cohesive force than that observed in younger
438 rubber plants and the control plots. The higher SOM content in older rubber plants was driven by
439 the higher cellulose content and lower lignin percentages in their FRL and MRL. Consequently,
440 rubber plants older than 11 years increased the soil cohesive force (with and without roots)
441 compared to younger rubber plants and the control, thereby enhancing aggregate stability and
442 reducing soil particle dispersion. These findings offer practical implications for managing rubber
443 plantations across different stand ages to restore soil quality in degraded tropical regions of Hainan
444 Island. For instance, younger stands may benefit from targeted organic amendments or
445 intercropping to accelerate SOM accumulation, while older stands might require interventions to
446 mitigate aggregate breakdown through root properties. The study underscores the role of root
447 systems in soil stability, suggesting that management practices promoting robust root development
448 regardless of variety could enhance aggregate cohesion and long-term productivity.

449 **Credit authorship contribution statement**

450 **WA:** Writing - original draft, visualization, Investigation, Data curation, formal analysis. **AM**
451 Investigation, Data curation. **TL:** visualization, formal analysis, **NK:** Writing – review & editing.
452 **AS:** Writing – review & editing. **KS:** Investigation, formal analysis. **QY:** Investigation, Funding

453 acquisition, review & editing. **HY:** Writing – review & editing, **WL:** Investigation, Data curation.
454 **WL:** Validation, Supervision, Resources, Conceptualization, Funding acquisition.

455 **Declaration of Competing Interest**

456 The authors declare that they have no known competing financial interests or personal
457 relationships that could have appeared to influence the work reported in this paper.

458 **Data availability**

459 Data will be made available on request.

460 **Acknowledgment**

461 This work was financially supported by the National Key Research and Development Program of
462 China (2021YFD2200403-04), Hainan Province Postdoctoral Research Project (RZ2500001086)
463 and the National Natural Science Foundation of China (No. 42367034 and 32160291).

464 **References**

465 Ali, W., Yang, M., Long, Q., Hussain, S., Chen, J., Clay, D., and He, Y.: Different fall/winter
466 cover crop root patterns induce contrasting red soil (Ultisols) mechanical resistance through
467 aggregate properties, *Plant and Soil*, 477, 461–474, <https://doi.org/10.1007/s11104-022-05430-4>,
468 2022.

469 Ali, W., Hussain, S., Chen, J., Hu, F., Liu, J., He, Y., and Yang, M.: Cover crop root-derived
470 organic carbon influences aggregate stability through soil internal forces in a clayey red soil,
471 *Geoderma*, 429, 116271, <https://doi.org/10.1016/j.geoderma.2022.116271>, 2023.

472 Barto, E. K., Alt, F., Oelmann, Y., Wilcke, W., and Rillig, M. C.: Contributions of biotic and
473 abiotic factors to soil aggregation across a land use gradient, *Soil Biology and Biochemistry*, 42,
474 2316–2324, <https://doi.org/10.1016/j.soilbio.2010.09.008>, 2010.

475 Chen, C., Liu, W., Jiang, X., and Wu, J.: Effects of rubber-based agroforestry systems on soil

476 aggregation and associated soil organic carbon: Implications for land use, *Geoderma*, 299, 13–24,
477 <https://doi.org/10.1016/j.geoderma.2017.03.021>, 2017.

478 Chen, J., Wu, Z., Zhao, T., Yang, H., Long, Q., and He, Y.: Rotation crop root performance and
479 its effect on soil hydraulic properties in a clayey Utisol, *Soil and Tillage Research*, 213, 105136,
480 <https://doi.org/10.1016/j.still.2021.105136>, 2021.

481 Deviren Saygin, S., Arı, F., Temiz, Ç., Arslan, Ş., Ünal, M. A., and Erpul, G.: Analysis of soil
482 cohesion by fluidized bed methodology using integrable differential pressure sensors for a wide
483 range of soil textures, *Computers and Electronics in Agriculture*, 191,
484 <https://doi.org/10.1016/j.compag.2021.106525>, 2021.

485 Elliott, E. T.: Aggregate Structure and Carbon, Nitrogen, and Phosphorus in Native and Cultivated
486 Soils, *Soil Science Society of America Journal*, 50, 627–633,
487 <https://doi.org/10.2136/sssaj1986.03615995005000030017x>, 1986.

488 Forster, M., Ugarte, C., Lamandé, M., and Faucon, M.-P.: Root traits of crop species contributing
489 to soil shear strength, *Geoderma*, 409, 115642, <https://doi.org/10.1016/j.geoderma.2021.115642>,
490 2022.

491 Halder, M., Liu, S., Zhang, Z. B., Guo, Z. C., and Peng, X. H.: Effects of residue stoichiometric,
492 biochemical and C functional features on soil aggregation during decomposition of eleven organic
493 residues, *CATENA*, 202, 105288, <https://doi.org/10.1016/j.catena.2021.105288>, 2021.

494 He, Y., Yang, M., Huang, R., Wang, Y., and Ali, W.: Soil organic matter and clay zeta potential
495 influence aggregation of a clayey red soil (Ultisol) under long-term fertilization, *Scientific Reports*,
496 11, 20498, <https://doi.org/10.1038/s41598-021-99769-w>, 2021.

497 He, Y., Wu, Z., Zhao, T., Yang, H., Ali, W., and Chen, J.: Different plant species exhibit
498 contrasting root traits and penetration to variation in soil bulk density of clayey red soil, *Agronomy*

499 Journal, 114, 867–877, <https://doi.org/10.1002/agj2.20972>, 2022.

500 Hok, L., de Moraes Sá, J. C., Boulakia, S., Reyes, M., de Oliveira Ferreira, A., Elie Tivet, F., Saab,
501 S., Aucaise, R., Massao Inagaki, T., Schimiguel, R., Aparecida Ferreira, L., Briedis, C., Santos
502 Canalli, L. B., Kong, R., and Leng, V.: Dynamics of soil aggregate-associated organic carbon
503 based on diversity and high biomass-C input under conservation agriculture in a savanna
504 ecosystem in Cambodia, CATENA, 198, 105065, <https://doi.org/10.1016/j.catena.2020.105065>,
505 2021.

506 Huang, M., Sun, S., Feng, K., Lin, M., Shuai, F., Zhang, Y., Lin, J., Ge, H., Jiang, F., and Huang,
507 Y.: Effects of *Neyraudia reynaudiana* roots on the soil shear strength of collapsing wall in
508 Benggang, southeast China, Catena, 210, 105883, <https://doi.org/10.1016/j.catena.2021.105883>,
509 2022

510 Kaiser, M. and Asefaw Berhe, A.: How does sonication affect the mineral and organic constituents
511 of soil aggregates? - A review, Journal of Plant Nutrition and Soil Science, 177, 479–495,
512 <https://doi.org/10.1002/jpln.201300339>, 2014.

513 Kamau, S., Barrios, E., Karanja, N. K., Ayuke, F. O., and Lehmann, J.: Dominant tree species and
514 earthworms affect soil aggregation and carbon content along a soil degradation gradient in an
515 agricultural landscape, Geoderma, 359, 113983, <https://doi.org/10.1016/j.geoderma.2019.113983>,
516 2020.

517 Kemper, W. D. and Rosenau, R. C.: Aggregate Stability and Size Distribution, in: Agronomy
518 Monograph, vol. 9, 425–442, <https://doi.org/10.2136/sssabookser5.1.2ed.c17>, 2018.

519 Kumar, A., Dorodnikov, M., Splettstößer, T., Kuzyakov, Y., and Pausch, J.: Effects of maize roots
520 on aggregate stability and enzyme activities in soil, Geoderma, 306, 50–57,
521 <https://doi.org/10.1016/j.geoderma.2017.07.007>, 2017.

522 Kurmi, B., Nath, A. J., Lal, R., and Das, A. K.: Water stable aggregates and the associated active
523 and recalcitrant carbon in soil under rubber plantation, *Science of the Total Environment*, 703,
524 135498, <https://doi.org/10.1016/j.scitotenv.2019.135498>, 2020.

525 Li, T., Hong, X., Liu, S., Wu, X., Fu, S., Liang, Y., Li, J., Li, R., Zhang, C., Song, X., Zhao, H.,
526 Wang, D., Zhao, F., Ruan, Y., and Ju, X.: Cropland degradation and nutrient overload on Hainan
527 Island: A review and synthesis, *Environmental Pollution*, 313, 120100,
528 <https://doi.org/10.1016/j.envpol.2022.120100>, 2022.

529 Liao, J., Yang, X., Dou, Y., Wang, B., Xue, Z., Sun, H., Yang, Y., and An, S.: Divergent
530 contribution of particulate and mineral-associated organic matter to soil carbon in grassland,
531 *Journal of Environmental Management*, 344, 118536,
532 <https://doi.org/10.1016/j.jenvman.2023.118536>, 2023.

533 Melo, T. R. de, Figueiredo, A., and Filho, J. T.: Clay behavior following macroaggregate
534 breakdown in Ferralsols, *Soil and Tillage Research*, 207, 104862,
535 <https://doi.org/10.1016/j.still.2020.104862>, 2021.

536 Nornadiyah Mohd Razali Yap Bee Wah: Power comparisons of Shapiro-Wilk, Kolmogorov-
537 Smirnov, Lilliefors and Anderson-Darling tests, *Journal of Statistical Modeling and Analytics*, 21–
538 33, 2011.

539 Oleghe, E., Naveed, M., Baggs, E. M., and Hallett, P. D.: Plant exudates improve the mechanical
540 conditions for root penetration through compacted soils, *Plant and Soil*, 421, 19–30,
541 <https://doi.org/10.1007/s11104-017-3424-5>, 2017.

542 Perović, V., Kadović, R., Đurđević, V., Pavlović, D., Pavlović, M., Čakmak, D., Mitrović, M., and
543 Pavlović, P.: Major drivers of land degradation risk in Western Serbia: Current trends and future
544 scenarios, *Ecological Indicators*, 123, 107377, <https://doi.org/10.1016/j.ecolind.2021.107377>,

545 2021.

546 Poirier, V., Roumet, C., Angers, D. A., and Munson, A. D.: Species and root traits impact
547 macroaggregation in the rhizospheric soil of a Mediterranean common garden experiment, *Plant
548 and Soil*, 424, 289–302, <https://doi.org/10.1007/s11104-017-3407-6>, 2018a.

549 Poirier, V., Roumet, C., and Munson, A. D.: The root of the matter: Linking root traits and soil
550 organic matter stabilization processes, *Soil Biology and Biochemistry*, 120, 246–259,
551 <https://doi.org/10.1016/j.soilbio.2018.02.016>, 2018b.

552 Prăvălie, R., Nita, I.-A., Patriche, C., Niculiță, M., Birsan, M.-V., Roșca, B., and Bandoc, G.:
553 Global changes in soil organic carbon and implications for land degradation neutrality and climate
554 stability, *Environmental Research*, 201, 111580, <https://doi.org/10.1016/j.envres.2021.111580>,
555 2021.

556 Rabot, E., Wiesmeier, M., Schlüter, S., and Vogel, H.-J.: Soil structure as an indicator of soil
557 functions: A review, *Geoderma*, 314, 122–137, <https://doi.org/10.1016/j.geoderma.2017.11.009>,
558 2018.

559 Rossi, L. M. W., Mao, Z., Merino-Martín, L., Roumet, C., Fort, F., Taugourdeau, O., Boukcim,
560 H., Fourtier, S., Del Rey-Granado, M., Chevallier, T., Cardinael, R., Fromin, N., and Stokes, A.:
561 Pathways to persistence: plant root traits alter carbon accumulation in different soil carbon pools,
562 *Plant and Soil*, 452, 457–478, <https://doi.org/10.1007/s11104-020-04469-5>, 2020.

563 Schad, P.: World Reference Base for Soil Resources—Its fourth edition and its history, *Journal of
564 Plant Nutrition and Soil Science*, 186, 151–163, <https://doi.org/10.1002/jpln.202200417>, 2023.

565 Shao, W., Zhang, Z., Guan, Q., Yan, Y., and Zhang, J.: Comprehensive assessment of land
566 degradation in the arid and semiarid area based on the optimal land degradation index model,
567 *CATENA*, 234, 107563, <https://doi.org/10.1016/j.catena.2023.107563>, 2024.

568 Shen, N., Wang, Z., Guo, Q., Zhang, Q., Wu, B., Liu, J., Ma, C., Delang, C. O., and Zhang, F.:
569 Soil detachment capacity by rill flow for five typical loess soils on the Loess Plateau of China,
570 *Soil and Tillage Research*, 213, 105159, <https://doi.org/10.1016/j.still.2021.105159>, 2021.

571 Smith, D. J., Wynn-Thompson, T. M., Williams, M. A., and Seiler, J. R.: Do roots bind soil?
572 Comparing the physical and biological role of plant roots in fluvial streambank erosion: A mini-
573 JET study, *Geomorphology*, 375, 107523, <https://doi.org/10.1016/j.geomorph.2020.107523>, 2021.

574 Sun, R., Wu, Z., Lan, G., Yang, C., and Fraedrich, K.: Effects of rubber plantations on soil
575 physicochemical properties on Hainan Island, China, *Journal of Environmental Quality*, 50, 1351–
576 1363, <https://doi.org/10.1002/jeq2.20282>, 2021.

577 Sun, R., Lan, G., Yang, C., Wu, Z., Chen, B., and Fraedrich, K.: Soil quality variation and its
578 driving factors within tropical forests on Hainan Island, China, *Land Degradation and*
579 *Development*, 34, 3418–3432, <https://doi.org/10.1002/ldr.4693>, 2023.

580 Team, R. C.: *a Language and Environment for Statistical Computing*, 2017.

581 Thomas, A., Bentley, L., Feeney, C., Lofts, S., Robb, C., Rowe, E. C., Thomson, A., Warren-
582 Thomas, E., and Emmett, B.: Land degradation neutrality: Testing the indicator in a temperate
583 agricultural landscape, *Journal of Environmental Management*, 346, 118884,
584 <https://doi.org/10.1016/j.jenvman.2023.118884>, 2023.

585 Vannoppen, W., Vanmaercke, M., De Baets, S., and Poesen, J.: A review of the mechanical effects
586 of plant roots on concentrated flow erosion rates, *Earth-Science Reviews*, 150, 666–678,
587 <https://doi.org/10.1016/j.earscirev.2015.08.011>, 2015.

588 Vannoppen, W., De Baets, S., Keeble, J., Dong, Y., and Poesen, J.: How do root and soil
589 characteristics affect the erosion-reducing potential of plant species?, *Ecological Engineering*, 109,
590 186–195, <https://doi.org/10.1016/j.ecoleng.2017.08.001>, 2017.

591 Walkley, A. and Black, I. A.: An examination of the degtjareff method for determining soil organic
592 matter, and a proposed modification of the chromic acid titration method, *Soil Science*, 37, 29–38,
593 <https://doi.org/10.1097/00010694-193401000-00003>, 1934.

594 Wang, B., Zhang, G.-H., Yang, Y.-F., Li, P.-P., and Liu, J.-X.: Response of soil detachment
595 capacity to plant root and soil properties in typical grasslands on the Loess Plateau, *Agriculture,
596 Ecosystems & Environment*, 266, 68–75, <https://doi.org/10.1016/j.agee.2018.07.016>, 2018a.

597 Wang, B., Zhang, G.-H., Yang, Y.-F., Li, P.-P., and Liu, J.-X.: The effects of varied soil properties
598 induced by natural grassland succession on the process of soil detachment, *CATENA*, 166, 192–
599 199, <https://doi.org/10.1016/j.catena.2018.04.007>, 2018b.

600 Wang, G., Huang, Y., Li, R., Chang, J., and Fu, J.: Influence of Vetiver Root System on
601 Mechanical Performance of Expansive Soil: Experimental Studies, *Advances in Civil Engineering*,
602 2020, 1–11, <https://doi.org/10.1155/2020/2027172>, 2020a.

603 Wang, G. Y., Huang, Y. G., Li, R. F., Chang, J. M., and Fu, J. L.: Influence of vetiver root on
604 strength of expansive soil-experimental study, *PLoS ONE*, 15, 1–20,
605 <https://doi.org/10.1371/journal.pone.0244818>, 2020b.

606 Wang, J., Wei, H., Huang, J., He, T., and Deng, Y.: Soil aggregate stability and its response to
607 overland runoff–sediment transport in karst peak–cluster depressions, *Journal of Hydrology*, 620,
608 129437, <https://doi.org/10.1016/j.jhydrol.2023.129437>, 2023.

609 Wuddivira, M. N., Stone, R. J., and Ekwue, E. I.: Clay, Organic Matter, and Wetting Effects on
610 Splash Detachment and Aggregate Breakdown under Intense Rainfall, *Soil Science Society of
611 America Journal*, 73, 226–232, <https://doi.org/10.2136/sssaj2008.0053>, 2009.

612 Wuddivira, M. N., Stone, R. J., and Ekwue, E. I.: Influence of cohesive and disruptive forces on
613 strength and erodibility of tropical soils, *Soil and Tillage Research*, 133, 40–48,

614 <https://doi.org/10.1016/j.still.2013.05.012>, 2013.

615 Xu, W., Liu, W., Tang, S., Yang, Q., Meng, L., Wu, Y., Wang, J., Wu, L., Wu, M., Xue, X., Wang,
616 W., and Luo, W.: Long-term partial substitution of chemical nitrogen fertilizer with organic
617 fertilizers increased SOC stability by mediating soil C mineralization and enzyme activities in a
618 rubber plantation of Hainan Island, China, *Applied Soil Ecology*, 182, 104691,
619 <https://doi.org/10.1016/j.apsoil.2022.104691>, 2023.

620 Yang, Q., Li, J., Xu, W., Wang, J., Jiang, Y., Ali, W., and Liu, W.: Substitution of Inorganic
621 Fertilizer with Organic Fertilizer Influences Soil Carbon and Nitrogen Content and Enzyme
622 Activity under Rubber Plantation, *Forests*, 15, 756, <https://doi.org/10.3390/f15050756>, 2024.

623 Yu, Z., Zheng, Y., Zhang, J., Zhang, C., Ma, D., Chen, L., and Cai, T.: Importance of soil
624 interparticle forces and organic matter for aggregate stability in a temperate soil and a subtropical
625 soil, *Geoderma*, 362, 114088, <https://doi.org/10.1016/j.geoderma.2019.114088>, 2020.

626 Yudina, A. and Kuzyakov, Y.: Dual nature of soil structure: The unity of aggregates and pores,
627 *Geoderma*, 434, 116478, <https://doi.org/10.1016/j.geoderma.2023.116478>, 2023.

628 Zhang, C.-B., Chen, L.-H., and Jiang, J.: Why fine tree roots are stronger than thicker roots: The
629 role of cellulose and lignin in relation to slope stability, *Geomorphology*, 206, 196–202,
630 <https://doi.org/10.1016/j.geomorph.2013.09.024>, 2014.

631 Zhu, X., Liu, W., Yuan, X., Chen, C., Zhu, K., Zhang, W., and Yang, B.: Aggregate stability and
632 size distribution regulate rainsplash erosion: Evidence from a humid tropical soil under different
633 land-use regimes, *Geoderma*, 420, 115880, <https://doi.org/10.1016/j.geoderma.2022.115880>,
634 2022.

635 Zou, X., Zhu, X., Zhu, P., Singh, A. K., Zakari, S., Yang, B., Chen, C., and Liu, W.: Soil quality
636 assessment of different *Hevea brasiliensis* plantations in tropical China, *Journal of Environmental*

637 Management, 285, 112147, <https://doi.org/10.1016/j.jenvman.2021.112147>, 2021.

638

639

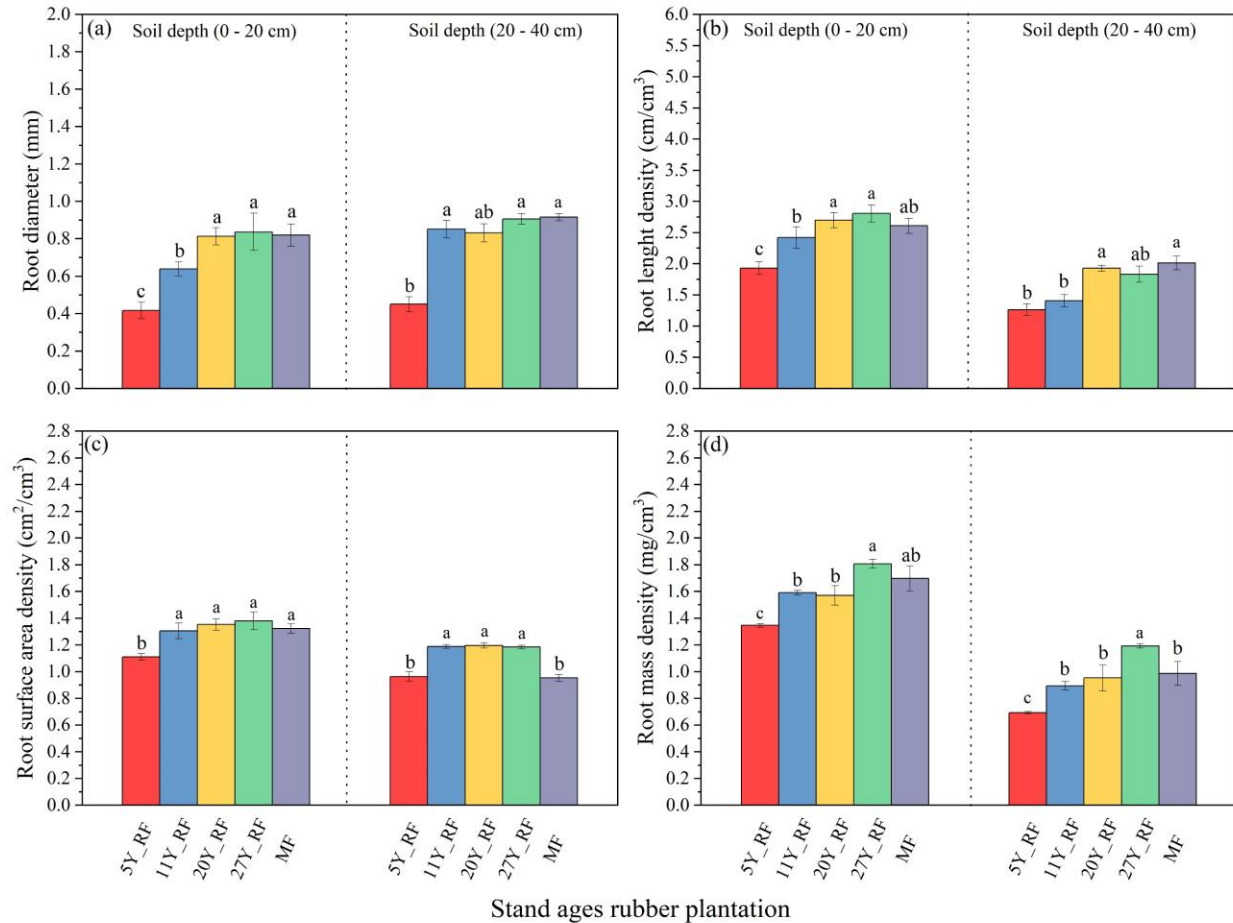
640 Table captions

641 **Table 1.** Basic physical and chemical characteristics of the experimental site.

Treatments	Soil depth (cm)	pH	BD (g/cm ³)	TOP (%)	SMC (%)	SOM (g/kg)	AN (mg/kg)	AP (mg/kg)	AK (mg/kg)
CK	0 -20	4.17	1.52	26.37	17.46	12.34	11.92	1.69	24.42
	20 - 40	4.21	1.56	23.26	15.25	11.36	11.45	1.56	18.15
5Y_RF	0 -20	4.37	1.39	28.39	19.25	20.98	11.63	2.79	34.62
	20 - 40	4.13	1.52	23.01	17.63	16.30	10.67	1.73	17.97
11Y_RF	0 -20	3.89	1.43	24.81	21.67	22.68	11.84	2.31	25.23
	20 - 40	4.02	1.51	23.1	20.77	20.56	10.42	1.7	16.44
20Y_RF	0 -20	4.08	1.36	24.98	21.41	23.37	10.67	2.33	29.02
	20 - 40	4.22	1.43	20.31	20.2	21.16	10.39	1.99	23.12
27Y_RF	0 -20	4.08	1.32	25.05	23.68	21.78	11.77	2.39	25.83
	20 - 40	4.26	1.41	25.24	19.9	21.04	10.17	1.84	18.92
MF	0 -20	4.42	1.31	29.52	22.76	21.20	13.47	1.81	36.15
	20 - 40	4.35	1.39	26.58	20.11	20.29	12.84	1.33	19.94

642 Note: CK: without forest plants; 5Y_RF: 5 years old rubber forest; 11Y_RF: 11 years old rubber forest; 20Y_RF: 20 years old
643 rubber forest; 27Y_RF: 27 years old rubber forest; MF: mix rubber forest with cinnamon trees; BD: Bulk density; TOP: Total
644 porosity; SMC: Soil moisture content; SOM: Soil organic matter; AN: Available nitrogen; AP: Available phosphorus; AK: Available
645 potassium.

646



647

648 **Figure 1.** Different stand-age rubber plantation root morphological properties with soil depths.

649 Each treatment was replicated three times ($n = 3$), and results are presented as mean \pm standard

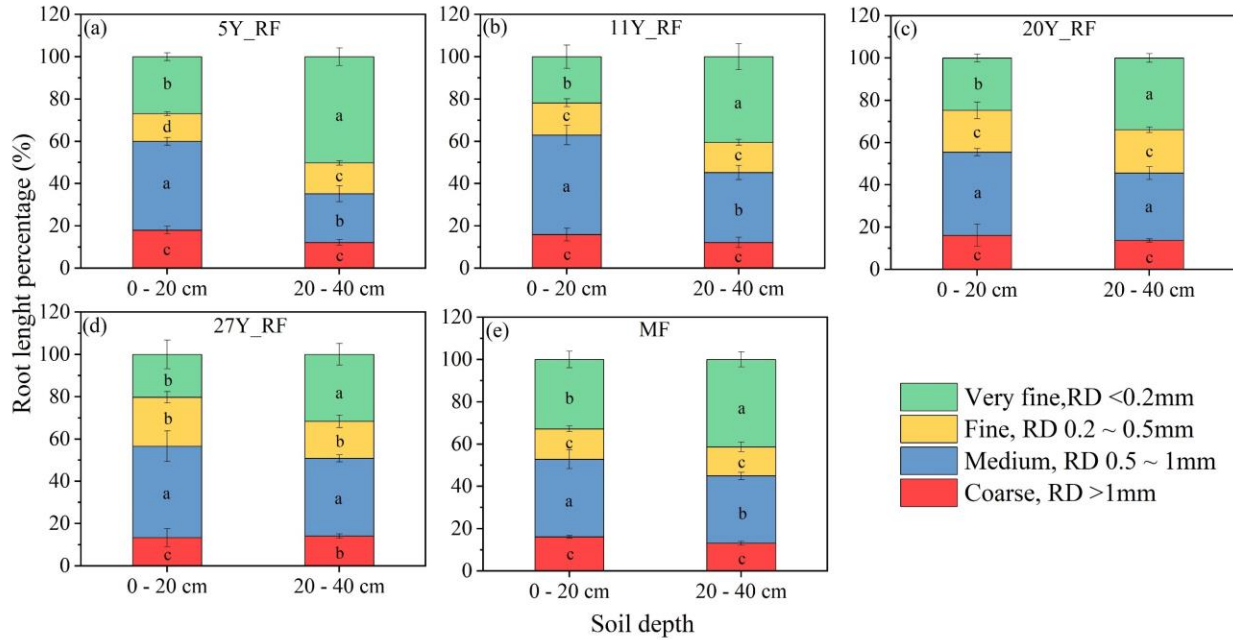
650 deviation. (a) Root diameter (RD), (b) Root length density (RLD), (c) Root surface area density

651 (RSD), and (d) Root mass density (RMD). Summary of ANOVA results of parameters presented

652 in supplementary table.1. CK: without forest plants; 5Y_RF: 5 years old rubber forest; 11Y_RF:

653 11 years old rubber forest; 20Y_RF: 20 years old rubber forest; 27Y_RF: 27 years old rubber forest;

654 and MF: mix rubber forest with cinnamon trees.



655

656

Figure 2. Root diameter distribution of rubber plants at different stand ages represented by the

657

root length percentage across four class diameters. Each treatment was replicated three times (n =

658

3), and results are presented as mean \pm standard deviation. Summary of ANOVA results of

659

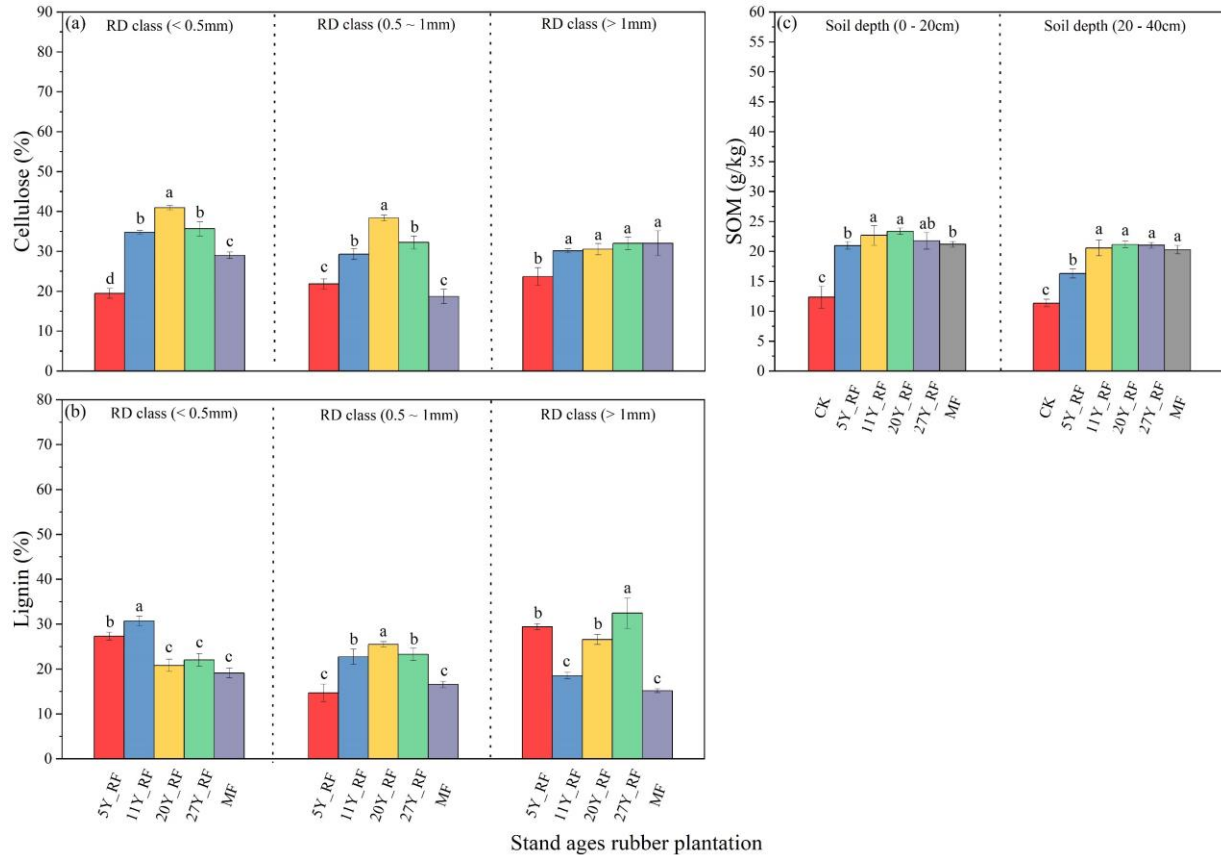
parameters presented in the supplementary table. 2. CK: without forest plants; 5Y_RF: 5 years old

660

rubber forest; 11Y_RF: 11 years old rubber forest; 20Y_RF: 20 years old rubber forest; 27Y_RF:

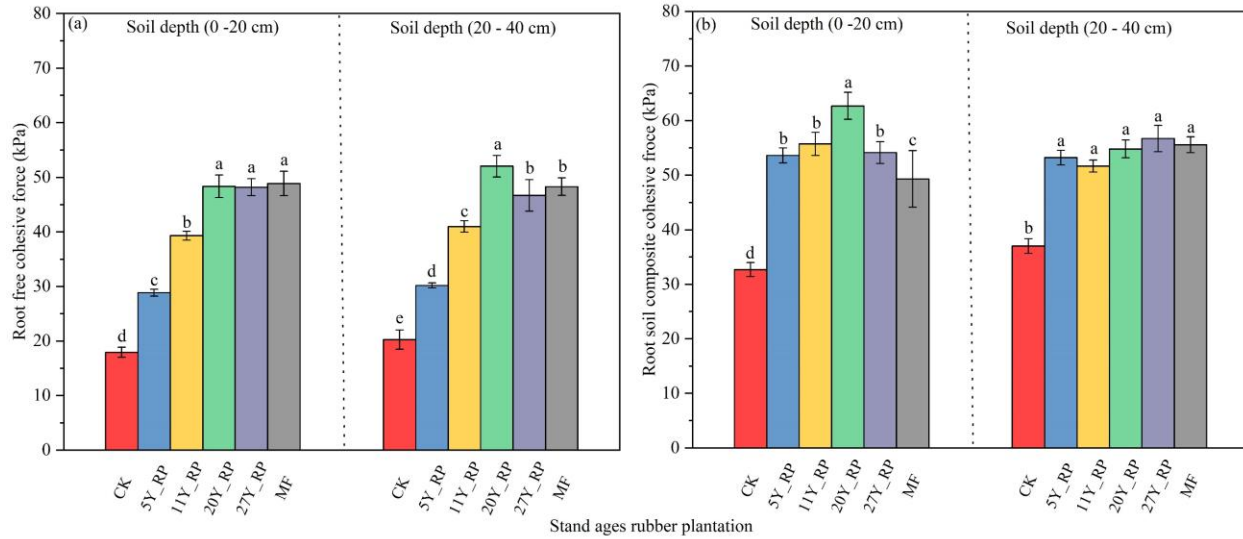
661

27 years old rubber forest; and MF: mix rubber forest with cinnamon trees.



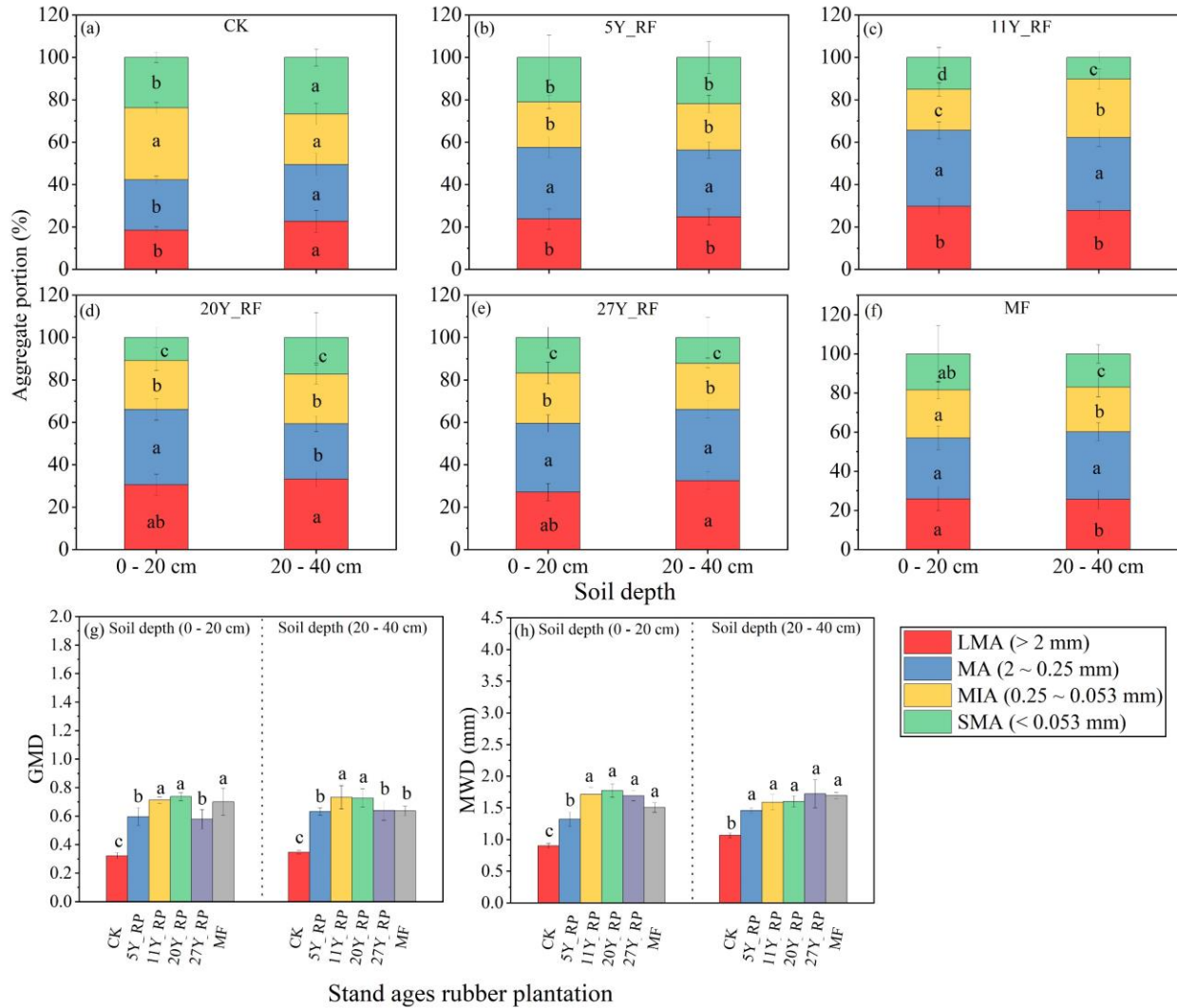
662

663 **Figure 3.** Different stand-age rubber plantation root chemical compositions and soil organic
 664 matter (SOM) distributions. Each treatment was replicated three times ($n = 3$), and results are
 665 presented as mean \pm standard deviation. (a) Cellulose, (b) Lignin, and (c) Soil organic matter
 666 (SOM). Summary of ANOVA results of parameters presented in the supplementary table. 3. CK:
 667 without forest plants; 5Y_RF: 5 years old rubber forest; 11Y_RF: 11 years old rubber forest;
 668 20Y_RF: 20 years old rubber forest; 27Y_RF: 27 years old rubber forest; and MF: mix rubber
 669 forest with cinnamon trees.



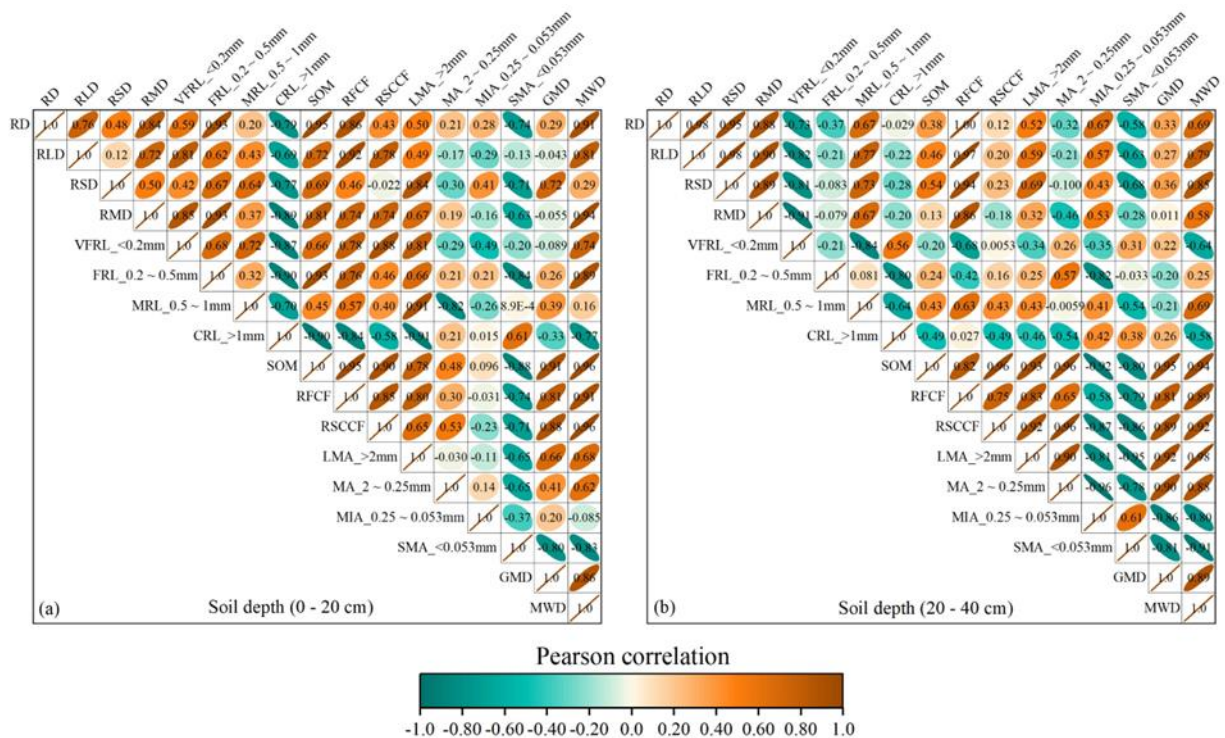
670

671 **Figure 4.** Soil cohesive force distribution under different stand-age rubber plantations. Each
 672 treatment was replicated three times ($n = 3$), and results are presented as mean \pm standard
 673 deviation (a) Root-free cohesive force (RFCS), (b) Root-soil composite cohesive force (RSCCF).
 674 Summary of ANOVA results of parameters presented in supplementary table .4. CK: without forest
 675 plants; 5Y_RF: 5 years old rubber forest; 11Y_RF: 11 years old rubber forest; 20Y_RF: 20 years
 676 old rubber forest; 27Y_RF: 27 years old rubber forest; and MF: mix rubber forest with cinnamon
 677 trees.



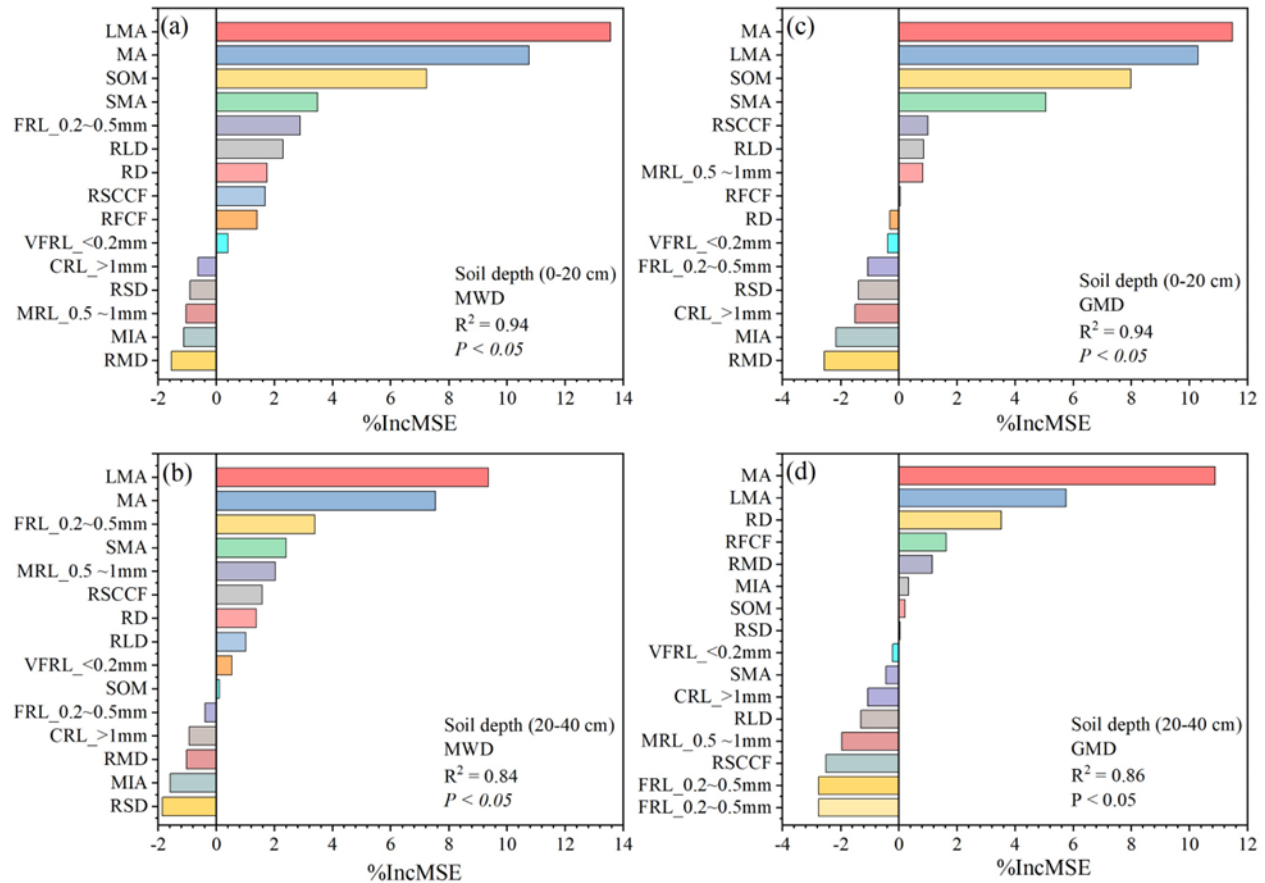
678

679 **Figure 5.** Different stand-age rubber plantation aggregate size distributions and soil aggregate
 680 stabilities (MWD and GWD) with soil depths. Each treatment was replicated three times ($n = 3$),
 681 and results are presented as mean \pm standard deviation. Summary of ANOVA results of parameters
 682 presented in supplementary table. 5. LMA: large macroaggregates; MA: macroaggregates; MIA:
 683 microaggregates; SMA: small microaggregates; CK: without forest plants; 5Y_RF: 5 years old
 684 rubber forest; 11Y_RF: 11 years old rubber forest; 20Y_RF: 20 years old rubber forest; 27Y_RF:
 685 27 years old rubber forest; and MF: mix rubber forest with cinnamon trees.



686

687 **Figure 6.** Pearson correlations ($P < 0.05$) for all root traits, aggregate stabilities, soil organic
 688 matter, and soil cohesive forces. RD: root diameter; RLD: root length density; RSD: root surface
 689 area density; RMD: root mass density; VFRL: very fine root length; FRL: fine root length; MRL:
 690 medium root length; CRL: coarse root length; SOM: soil organic matter; RFCF: root-free cohesive
 691 force; RSCCF: root–soil composite cohesive force; LMA: large macroaggregates (> 2 mm); MA:
 692 macroaggregates (2–0.25 mm); MIA: microaggregates (0.25–0.053 mm); SMA: small
 693 microaggregates (< 0.053 mm); GMD: geometric mean diameter; MWD: mean weight diameter.
 694 The dark brown color indicates a positive correlation, and the pine green color indicates a negative
 695 correlation.



696

697 **Figure 7.** Random forest model ($P < 0.05$) to identify the key predictors of mean weight diameter

698 (MWD) and geometric mean diameter (GMD). RD: root diameter; RLD: root length density; RSD:

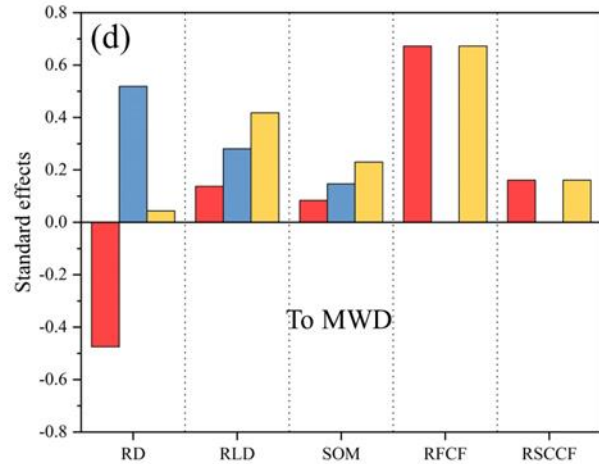
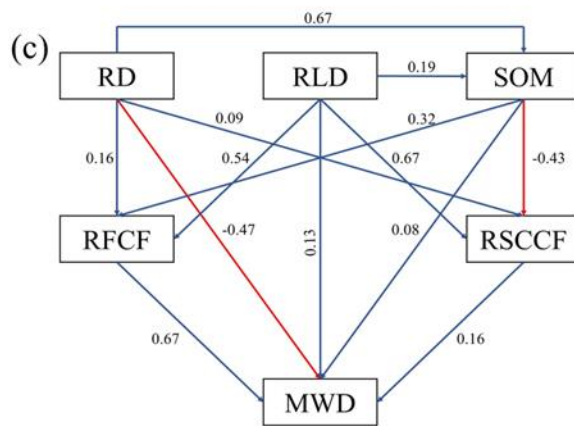
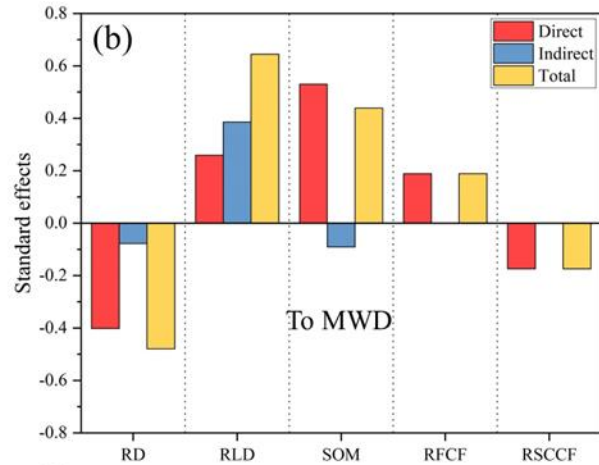
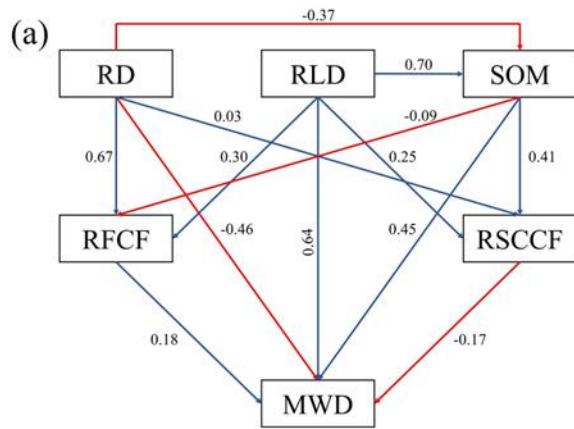
699 root surface area density; RMD: root mass density; VFRL: very fine root length; FRL: fine root

700 length; MRL: medium root length; CRL: coarse root length; SOM: soil organic matter; RFCF root-

701 free cohesive force; RSCCF: root–soil composite cohesive force; LMA: large macroaggregates (>

702 2 mm); MA: macroaggregates (2–0.25 mm); MIA: microaggregates (0.25– 0.053 mm); SMA:

703 small microaggregates (< 0.053 mm).



704

705 **Figure 8.** Partial least squares-path models (PLS-PM) ($P < 0.05$) indicating the indirect and direct
 706 impact of root properties, soil organic matter, and cohesive forces on soil aggregate stability at 0–
 707 20 cm (a, and b) and 20–40 cm (c, and d). The numbers near the arrows are standardized path
 708 coefficients. The blue line indicates the positive direction, and the red line indicates the negative
 709 direction. RD: root diameter; RLD: root length density; SOM: soil organic matter; RFCF: root-
 710 free cohesive force; RSCCF: root–soil composite cohesive force; MWD: mean weight diameter.